

Research Paper

Simulation study of competitive adsorption of CH₄/CO₂ and CH₄/N₂ in anthracite coal

Gang Bai^{a,c,1,*}, Haijing Zhang^b, Xun Zhang^b, Chaojun Fan^b, Jue Wang^a, Jie Wei^d, Yilong Zhang^{a,c}

^a College of Safety Science & Engineering, Liaoning Technical University, Huludao, Liaoning 125105, China

^b College of Mining, Liaoning Technical University, Fuxin 123000, China

^c Key Laboratory of Mine Thermodynamic Disasters & Control of Ministry of Education, Huludao, Liaoning 125105, China

^d China Academy of Safety Science and Technology, Beijing 100012, China

ARTICLE INFO

Keywords:

Anthracite

Competitive adsorption

Coalbed methane (CBM)

ABSTRACT

This study investigated the adsorption properties of gas molecules in coal seams, which are crucial for gas injection in enhanced coalbed methane recovery (ECBM). Competitive adsorption simulations of CH₄, CO₂, and N₂ single-component gases and various CH₄/CO₂ and CH₄/N₂ mixing ratios were conducted using an anthracite coal model from the Zhao Zhuang coal mine. Grand Canonical Monte Carlo (GCMC) simulations were performed at a system temperature of 298 K and pressures ranging from 0.1 to 5 MPa to explore the mechanism by which injected CO₂ and N₂ replaced CH₄ in the coal seam. The results indicated that CO₂ exhibited a significantly higher inhibitory effect on CH₄ than on N₂ at the same ratio. As the ratio of N₂ increased, the inhibition of CH₄ became more pronounced. When the CH₄/N₂ ratio exceeded 1:3, CH₄ was at a disadvantage in terms of competitive adsorption, with the coal's adsorption capacity of N₂ surpassing that of CH₄. This suggested that the amount of N₂ injected was critical for effectively displacing CH₄ from the coal seam. During competitive adsorption, the gas mixture ratio had a minimal impact on the potential energy distribution and adsorption selectivity coefficients, which consistently favored CO₂ adsorption over CH₄, and CH₄ adsorption over N₂. The van der Waals energy generated during competitive adsorption of CH₄/CO₂ was twice that of CH₄/N₂. Based on these findings, an optimized scheme incorporating CO₂-ECBM and N₂-ECBM technologies was proposed to provide theoretical guidance for gas injection in Enhanced Coalbed Methane Recovery (ECBM) and reduce the cost of coalbed methane (CBM) recovery.

1. Introduction

Driven by the dual-carbon target, the coal industry needs to transition and innovate to achieve carbon reduction and efficient resource utilization. With its extensive and widely distributed coal mines, China possesses substantial coalbed methane reserves as an unconventional natural gas resource, characterized by abundant availability and low cost. However, the deep burial and low permeability of China's coal seams significantly hinders the efficiency of coalbed methane recovery (Long et al., 2021a; Wang et al., 2012; Bai et al., 2022). Gas injection has emerged as a sustainable green technology for enhanced coalbed methane recovery that relies on the competitive adsorption properties of gases in coal (Long et al., 2021a). A comprehensive study of these

properties is essential to optimize gas injection strategies, increase coalbed methane recovery rates, lower recovery costs, and promote efficient resource utilization. Such advancements are critical for supporting emission reduction targets and sustainable energy practices.

In recent years, CO₂-ECBM and N₂-ECBM have emerged as widely studied methods for enhancing coalbed methane recovery. Three stages in the CO₂-ECBM process of raw coal are identified, which can be influenced by coal pore topological characteristics: replacement dominates initially, followed by a combination of replacement, carry-over, and dilution in the middle stage, and carry-over and weakening in the final stage (Liu, 2023). Using nuclear magnetic resonance (NMR) technology, injecting CO₂ after depressurization of conventional coal reservoirs improves methane desorption efficiency. Moreover, the CH₄

* Corresponding author at: College of Safety Science & Engineering, Liaoning Technical University, Huludao, Liaoning 125105, China.

E-mail address: baigang@lntu.edu.cn (G. Bai).

¹ ORCID: 0000-0002-4599-6388.

displacement rate by CO_2 decreases rapidly during the early phase of injection and then slows until reaching the competitive adsorption equilibrium (Zheng et al., 2022). Numerical simulations have revealed that the gas concentration, flow rate, and permeability are proportional to the injection pressure. Additionally, nitrogen injection can enhance methane desorption by increasing pressure gradients and permeability, whereas permeability decreases as the outlet pressure approaches atmospheric levels, reflecting interactions between pressure, seepage, and stress deformation (Liu et al., 2024). Furthermore, higher gas diffusivity in coal can improve both CO_2 injection rates and CH_4 recovery efficiency (Sun et al., 2018). Gas competition for adsorption sites at various temperatures can drive CH_4 desorption during CO_2 and N_2 injection (Yang et al., 2021a, 2021b). Finally, injecting CH_4/N_2 mixtures has been proven to reduce formation swelling and enhance both CH_4 recovery and CO_2 sequestration compared with pure CO_2 injection (Zhang et al., 2020). It has been experimentally demonstrated that CH_4 recovery rates can reach 71 % for N_2 -ECBM and 86 % for CO_2 -ECBM when the molar percentage of CH_4 is 10 %. This demonstrates a moderate increase in coal permeability with N_2 injection, whereas CO_2 injection significantly reduces coal permeability (Zhou et al., 2013). The CO_2 selectivity in adsorption can be influenced by temperature, pressure, and volume mole fraction, with the selectivity decreasing at higher pressures and self-fractions but increasing with temperature (Dong et al., 2019). The CO_2 adsorption capacity can be 2–2.63 times greater than CH_4 , with higher coal ranks enhancing the CO_2 adsorption in CH_4/CO_2 competitive adsorption (Asif et al., 2019). The adsorption and transport of CH_4/CO_2 in coal ultramicropores are temperature dependent, and the adsorption increases as the volume mole fraction increases. CO_2 exhibits superior adsorption and diffusion properties compared to CH_4 , and coal gas wettability can be identified as a key factor for CO_2 sequestration and CH_4 recovery efficiency (Zhao et al., 2016). Coal wettability was analyzed to determine the descending order of wetting as CO_2 , CH_4 , and N_2 (Saghafi et al., 2014). The superior CO_2 adsorption over CH_4 and N_2 was determined using chromatographic techniques and lattice density functional theory study of the Ono-Kondo equation (Ottiger et al., 2008). High CO_2 concentrations have been identified to inhibit the competitive adsorption of CH_4 , CO_2 , and N_2 in coal (Long et al., 2021a). CH_4/CO_2 competitive adsorption experiments on shale have suggested that injecting small amounts of CO_2 can significantly increase the adsorption of gas mixtures while suppressing CH_4 adsorption (Du et al., 2020). Three regions of gas adsorption dynamics were identified: fast decay, slow decay, and adsorption equilibrium. Before reaching adsorption equilibrium, the gas adsorption rates are higher at elevated temperatures than at lower temperatures (Sun et al., 2021). Under specific conditions, higher CO_2 concentrations reduce the CO_2/CH_4 adsorption selectivity in coal (Zhang et al., 2015). The competitive adsorption of CH_4 , CO_2 , and N_2 in deep coal seams has been explored using a coal supercell model, concluding that CO_2/N_2 injection cannot enhance CH_4 desorption as the coal pore size increases (Yang et al., 2020). Coal rank and moisture have been reported to significantly affect the CH_4/CO_2 competitive adsorption, with higher coal rank increasing adsorption capacity and moisture reducing it (Li et al., 2019). These studies have primarily examined the factors influencing CH_4/CO_2 and CH_4/N_2 adsorption, confirming that CO_2 -ECBM is more effective than N_2 -ECBM, with higher CO_2 concentrations inhibiting CH_4/CO_2 adsorption. However, the effects of gas concentration on the CH_4/N_2 competitive adsorption mechanisms require further research. In addition, existing studies lack clarity in distinguishing potential energy from interaction energy during adsorption energy changes, and analyses of potential energy fail to fully elucidate the reaction mechanisms. Finally, there is limited research that leverages competitive adsorption properties to optimize gas injection strategies for coalbed methane extraction.

This study comprehensively analyzed the effect of gas mixture ratios on the competitive adsorption of CH_4/CO_2 and CH_4/N_2 using the Grand Canonical Monte Carlo (GCMC) simulation method using Materials Studio software. The analysis of different gas mixture proportions

highlights the distinction between potential energy and intermolecular interaction energy during competitive adsorption, revealing the nature of the potential energy reaction. Based on these findings, optimization schemes for CO_2 -ECBM and N_2 -ECBM technologies were proposed to reduce the cost of CBM recovery. The results of this study not only enhance the understanding of the competitive adsorption mechanism of gas mixtures but also offer valuable guidance for selecting optimal gas injection ratios, particularly for CO_2 - and N_2 -driven gases, in the practical application of gas injection technology for coalbed methane (CBM) replacement.

2. Simulation methods and theory

2.1. Molecular modelling

Coal is formed over millions of years through biological and geological processes, including chemical elements such as C, H, O, N, and S. Its internal structure is irregular because of geological effects during formation and is characterized by a graphite-like layered structure of thin, parallel layers interconnected by van der Waals forces and other interactions. The coal matrix contains numerous pores and fissures, which endow it with adsorption properties. Functional groups, such as hydroxyl, ether bonds, ketone groups, and carboxyl groups, are integral to the chemical and combustion properties of coal. Accurate coal molecular models are essential to obtain reliable simulation results. Over time, macromolecular models, such as the Fuchs, Given, Wiser, and Shinn models (Shinn, 1984; Jia et al., 2023a), have been developed. In this study, a molecular model of anthracite from the Zhaozhuang coal mine with a molecular formula of $\text{C}_{243}\text{H}_{202}\text{N}_2\text{O}_7\text{S}$ and molecular weight of 3290 was adopted as the structural unit. The elemental composition of the model was C (88.632 %), H (6.140 %), N (0.851 %), O (3.404 %), and S (0.973 %).

2.2. Model optimization and parameter setting

The objective of model optimization was to achieve a more reasonable geometric configuration by adjusting the molecular bond energies and bond angles, thereby avoiding the irrational spatial arrangements that could affect the material's physical properties. This process reduced the total energy of the model to develop a more structurally stable 3D configuration, with the lowest energy structure identified as the optimal configuration. Model optimization was performed using the Force module in Materials Studio software, encompassing geometry optimization, annealing treatment, and molecular dynamics optimization. For geometry optimization, the COMPASS force field, force-field-assigned charges, medium accuracy, and smart algorithm were applied to reduce the total energy of the coal molecule. To avoid local optimization, 10 annealing cycles were conducted within the temperature range of 300–500 K to further minimize energy consumption. Subsequently, in the Amorphous Cell module, six anthracite molecules were used as basic units with periodic boundary conditions to constrain cell construction. The cell was geometrically optimized and annealed again following the same steps and then subjected to NVT system synthesis using the Nose temperature control method for molecular dynamics optimization. The final coal cell model with the lowest total energy was selected as the optimal conformation. Fig. 1 presents the molecular models of coal and coal cells before and after optimization. Additionally, the adsorbent molecules (CO_2 , CH_4 , and N_2) underwent geometric optimization, annealing treatment, and dynamic optimization to identify their optimal configurations, using parameters consistent with those for coal molecules. Owing to the simplicity of the adsorbate molecular structure, the visible surface changes before and after optimization were minimal. However, adjustments in bond energies and bond angles during optimization reduced the total energy, stabilizing the adsorbate models. The optimized molecular model of the adsorbate is shown in Fig. 2.

The energy changes in the molecular structure of coal before and

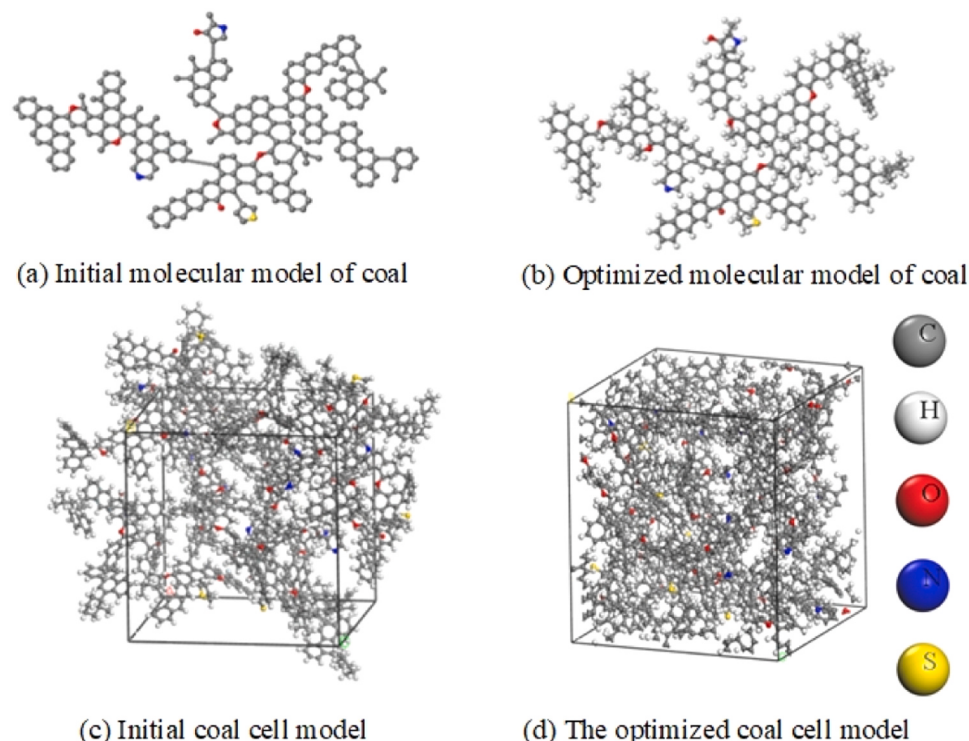


Fig. 1. Molecular model of coal and coal cells before and after optimization.

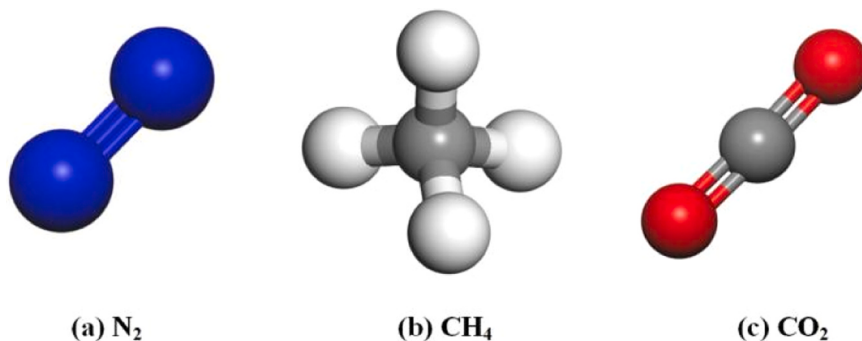


Fig. 2. Optimized gas molecular model.

after optimization are summarized in [Table 1](#). The total energy of the model decreased significantly, with reductions of 184,867.657 kcal/mol in van der Waals energy, 6094.181 kcal/mol in bond stretching energy, and 236.767 kcal/mol in electrostatic energy. These reductions indicated that the overall energy decrease primarily resulted from changes in the bond stretching, van der Waals, and electrostatic energies. Conversely, increases were observed in the bond angle, torsion, and reversal energies, suggesting that the spatial structure of the coal molecular model underwent significant changes during optimization. These changes, achieved through molecular mechanics and molecular dynamics, resulted in a more pronounced bending of the overall structure.

2.3. Coal cell density selection

Density is a fundamental physical property of coal and serves as a critical criterion for evaluating the reasonableness of structural coal models. By applying periodic boundary conditions, the optimal density of coal molecules can be determined. This process can be conducted in the Amorphous Cell module of Materials Studio molecular simulation software. In this study, the density values were incrementally increased from 0.5 to 1.7 in 0.05 g/cm^3 steps. The force field, charge, and accuracy settings were consistent with those of previous configurations. The optimal density of the coal model was identified by analyzing the

Table 1
Energy changes before and after optimization of the coal macromolecule model.

	Total energy (kcal/mol)	Valence electron energy (kcal/mol)				Non-bonding energy (kcal/mol)		
		Bond stretching energy	Bond angle energy	Torsional energy	Inversion energy	Hydrogen bonding energy	Van der Waals energy	Electrostatic energy
Initiate	205,835.255	6419.711	407.345	7930.275	8.444	0.000	185,683.647	208.055
Finally	9206.881	325.530	588.377	7996.156	36.817	0.000	815.990	- 28.712

relationship between the potential energy and density, enabling the determination of the model's cell size.

The relationship between the potential energy and the density of the coal macromolecule model is shown in Fig. 3. The potential energy reached its lowest value at a density of 1.05 g/cm^3 and increased again at 1.3 g/cm^3 . According to established practices (Han et al., 2018; Meng et al., 2018; Takanohashi et al., 2000; Qu et al., 2023), the density of a coal structure model is typically the value at the second local potential energy minimum, after the first. Therefore, the simulated density of the coal cell was determined to be 1.3 g/cm^3 . Literature indicates that the measured density of real-world anthracite coal ranges from 1.4 to 1.5 g/cm^3 (Diamond, 1957). The slightly lower simulated density can result from the exclusion of the mineral content in the model, as the minerals are not incorporated into the coal molecular structure (Meng et al., 2018; Sun et al., 2022). This omission minimally affects the adsorption properties because they are primarily governed by the structure and pore characteristics of organic matter, with minerals having a relatively limited influence. Thus, the coal molecular model was suitable for simulating the competitive adsorption of gas mixtures in anthracite coal. The final cell dimensions were $A = B = C = 3.36 \text{ nm}$ and $\alpha = \beta = \gamma = 90^\circ$.

This study revealed that water molecules can interact strongly with the functional groups on the coal surface, leading to preferential adsorption, which significantly reduces the total adsorption capacity of CO_2 , CH_4 , and N_2 on coal. This interaction also inhibits gas desorption and diffusion, thereby decreasing the risk of gas accumulation (Xiang et al., 2014; Yang et al., 2021a, 2021b). Conversely, in the dry coal samples, the adsorption sites were fully exposed, allowing the gas adsorption capacity of the coal to reach its limit with minimal restrictions on gas desorption and diffusion. Using dry coal samples for the simulation helps model the most severe gas accumulation scenarios that could occur in coal mines, thereby providing a scientific basis for devising effective safety measures. Consequently, the coal molecular model in this study excluded the effect of moisture content.

2.4. Simulation scenarios and parameter settings

This study simulated the competitive adsorption of single-component gases (CO_2 , CH_4 , and N_2) and their mixtures at various ratios (1:1, 1:2, 1:3, and 1:4) of CH_4/CO_2 and CH_4/N_2 in coal using the Grand Canonical Monte Carlo (GCMC) method. Simulations were conducted at a system temperature of 298 K and pressures ranging from 0.1

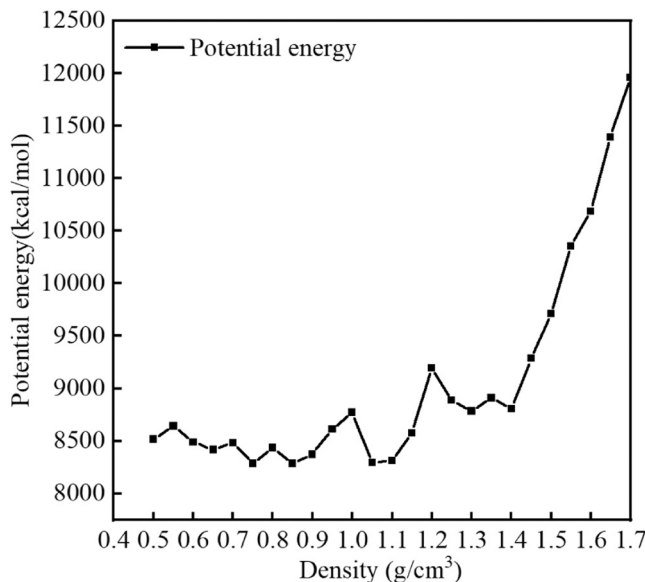


Fig. 3. Potential energy density diagram of coal molecular model.

to 5 MPa . The adsorption isotherms, potential energies, interaction energies, and density distributions of single-component gases and gas mixtures were obtained. The COMPASS force field was selected for the simulation based on its superior accuracy in modeling gas adsorption in porous media, such as coal, as demonstrated in previous studies (You et al., 2016; Babatunde et al., 2021; Mcquaid et al., 2004). The simulation parameters included the equilibration and production steps set at 1×10^6 , the fugacity steps set at 20, the system temperature fixed at 298 K , and the charge assignment based on the Forcefield assigned. The Ewald method was adopted to calculate the interatomic electrostatic interaction energy, whereas the van der Waals energy was calculated using the atom-based method with a truncation distance of 12.5 Å .

The gas adsorption units obtained from the simulations in this study were expressed as /u.c., which represents the number of gas molecules adsorbed per unit of coal molecules. However, in physical experiments, the most commonly used unit was cm^3/g . Consequently, conversion was required, which was performed using Eq. (1):

$$\text{STPcm}^3/\text{g} = 10^3 \times V_{\text{mol}} \times N/M \quad (1)$$

where N is the number of adsorbed molecules; M is the molar mass of a single crystal cell, g/mol ; and V_{mol} is the molar volume of the gas under standard conditions, $V_{\text{mol}} = 22.4 \text{ L/mol}$.

3. Results and discussion

3.1. Adsorption capacity

3.1.1. Laws of adsorption of single-component gases by coal

To clearly understand the adsorption behavior of mixed gases in coal, it is essential to first examine the adsorption patterns of individual gases to provide a foundation for analyzing mixed gas adsorption. In this study, the adsorption of single-component gases CH_4 , CO_2 , and N_2 in coal was simulated, and their respective adsorption isotherms are presented in Fig. 4.

Fig. 4 illustrates that the maximum adsorption capacities of CO_2 , CH_4 , and N_2 were 146.595 , 92.125 , and $63.649 \text{ cm}^3/\text{g}$, respectively, indicating that coal exhibited the highest adsorption capacity for CO_2 , followed by CH_4 , with N_2 being the lowest. As the pressure increased, the adsorption curves demonstrated that the gas adsorption increased rapidly at low pressures but slowed significantly at higher pressures,

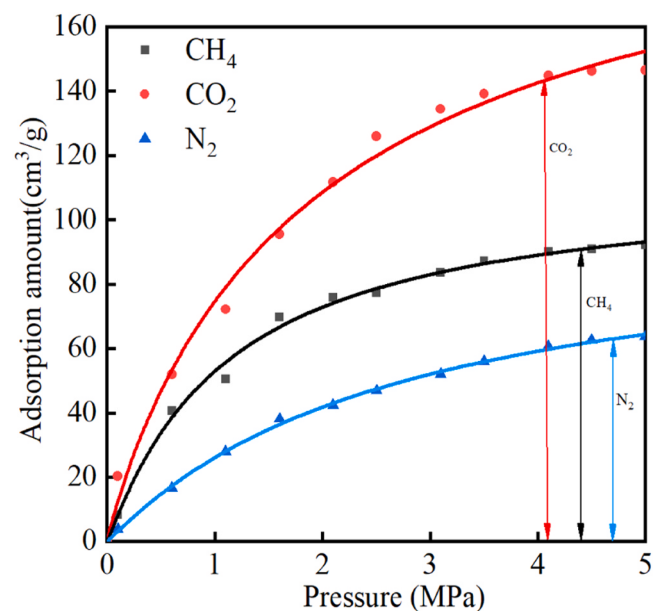


Fig. 4. Pure CO_2 , CH_4 , and N_2 adsorption isotherms.

whereas the adsorption amount continued to increase. This behavior could be because at low pressure, the gas molecules rapidly occupied the medium and large pores of coal, whereas at higher pressures, the gas molecules accelerated and occupied smaller pores. However, the limited number of adsorption sites in coal reduced the adsorption rate. CO_2 , the smallest molecule, penetrated the coal micropores more efficiently than CH_4 and N_2 . The simulation results were compared with the findings of Wu et al., who investigated the adsorption behavior of CO_2 , CH_4 , and N_2 through molecular simulations (Yang et al., 2020; Wu et al., 2019; Long et al., 2021b), and the experimental data from Xiao et al. (2023), Pini et al. (2009). The high consistency between the two validates the reliability and scientific accuracy of this study, demonstrating the credibility of the simulation methods and results, which provide valuable insights for reference.

3.1.2. Gas mixture adsorption

The adsorption trends of gases in the CH_4/CO_2 and CH_4/N_2 mixture systems with increasing pressure were aligned with those observed for the corresponding single-component gases (Jia et al., 2023a). Fig. 5 illustrates the adsorption isotherms for CH_4/CO_2 mixtures at different ratios, indicating that as the proportion of CO_2 in the mixture increased, CO_2 adsorption by coal continued to increase, while CH_4 adsorption decreased. Similarly, Fig. 6 shows the adsorption isotherms of the CH_4/N_2 mixtures at various ratios. When the CH_4/N_2 ratio was less than 1:3, CH_4 adsorption remained higher than N_2 adsorption. At a 1:3 ratio, CH_4 and N_2 adsorption was approximately equal. Beyond this ratio, N_2 adsorption surpassed CH_4 adsorption, indicating that N_2 was the dominant adsorbate in the competitive adsorption process. This shift demonstrated that at a CH_4/N_2 ratio of 1:3, the originally weaker adsorbable gas, N_2 , exceeded CH_4 , which previously had stronger adsorption, establishing dominance in subsequent competitive adsorption.

Fig. 7 illustrates the proportion of single-component gas adsorption in the CH_4/CO_2 mixtures at various ratios. CO_2 adsorption dominated CH_4 adsorption during the competitive adsorption process. As the proportion of injected CO_2 increased, CO_2 adsorption increased, while CH_4 adsorption decreased, indicating an inhibitory effect of CO_2 on CH_4 adsorption. Similarly, Fig. 8 shows the adsorption proportions of CH_4/N_2 mixtures at different ratios. During the CH_4/N_2 competitive adsorption process, the CH_4 adsorption gradually decreased, while the N_2 adsorption increased as the proportion of injected N_2 increased. When

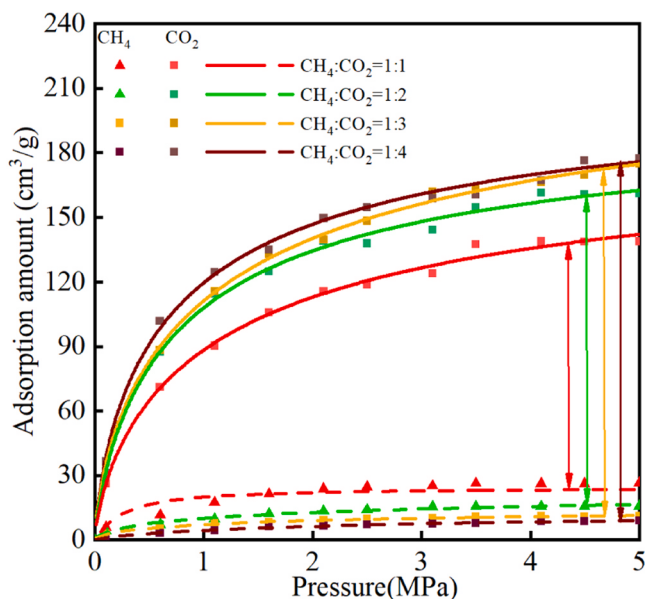


Fig. 5. CH_4/CO_2 adsorption isotherms.

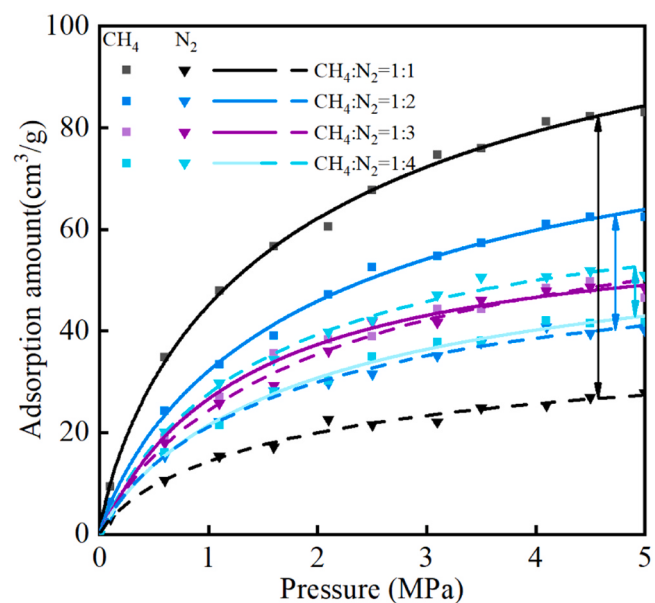


Fig. 6. CH_4/N_2 adsorption isotherms.

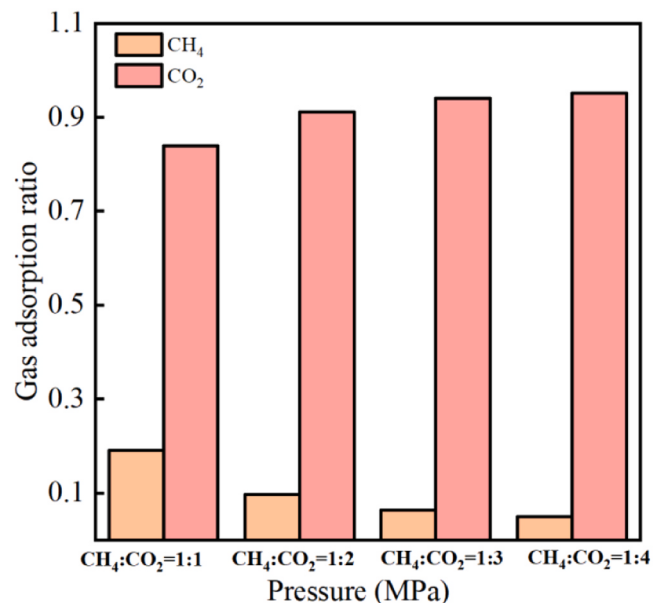


Fig. 7. Percentage adsorption of each gas in CH_4/CO_2 .

the CH_4/N_2 ratio reached 1:3, N_2 adsorption slightly exceeded CH_4 adsorption, demonstrating that the N_2 content affected the competitive adsorption between CH_4 and N_2 .

In summary, coal exhibited consistently stronger adsorption of CO_2 than CH_4 . In the competitive adsorption of CH_4 and N_2 , the adsorption capacity of coal was significantly affected by the N_2 content. Higher ratios of injected N_2 resulted in more pronounced inhibition of CH_4 adsorption. This indicated the importance of monitoring N_2 levels during its application to displace CH_4 in coal beds to ensure effective extraction. Additionally, both CO_2 and N_2 inhibited CH_4 adsorption, and the inhibitory effect of CO_2 was markedly stronger. This demonstrated that CO_2 injection is more effective than N_2 injection in the coalbed methane replacement technology.

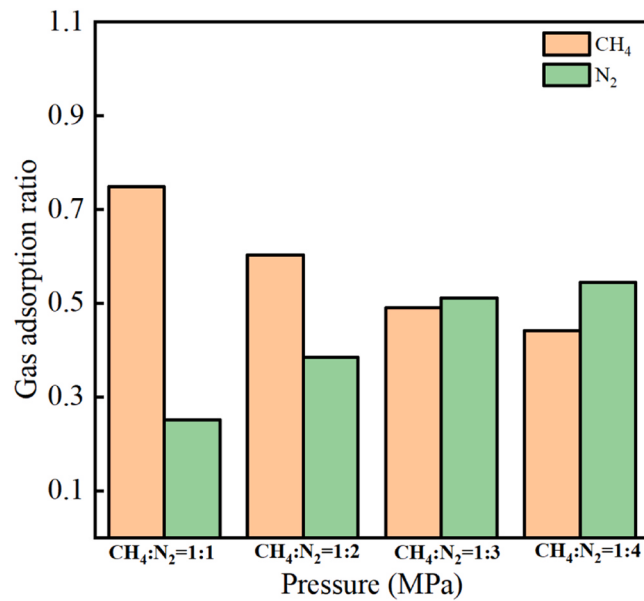


Fig. 8. Percentage adsorption of each gas in CH₄/N₂.

3.2. Potential energy distribution

The potential energy distribution reflects the probability that an adsorbate occupies an adsorption site within an adsorbent based on the potential energy response and is instrumental in analyzing adsorption site information during competitive adsorption. Fig. 9 illustrates the energy distribution for coal adsorption of the single-component gases CO₂, CH₄, and N₂. The peak potential energies were – 6.25 kcal/mol for CO₂, – 4.25 kcal/mol for CH₄, and – 3.25 kcal/mol for N₂. Higher absolute values of the potential energy indicated stronger intermolecular forces, favoring the occupation of adsorption sites (Wu et al., 2019b). The order of the absolute values of the potential energy of coal for these gases was CO₂ > CH₄ > N₂, with CO₂ exhibiting the lowest peak value and N₂ the highest. This demonstrated that CO₂ was more likely to occupy the preferential adsorption sites. Consequently, the adsorption capacity of coal for the gases followed the order of CO₂ > CH₄ > N₂.

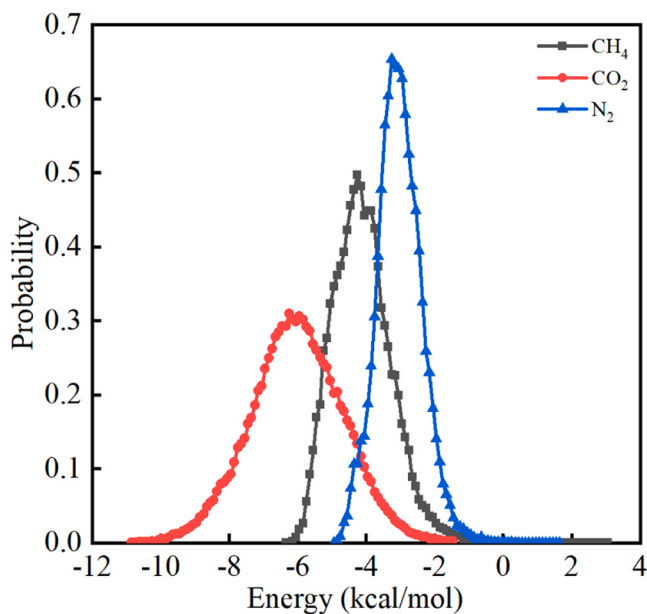


Fig. 9. Potential energy distribution of coal adsorption of pure CO₂, CH₄, and N₂.

The energy distributions of the CH₄/CO₂ mixtures with different ratios are shown in Fig. 10. The data indicated that the potential energies of CH₄ and CO₂ remained relatively stable across different ratios, with the optimal adsorption site potential energy for CO₂ ranging from – 6.45 to – 6.15 kcal/mol, and for CH₄ from – 5.05 to – 4.25 kcal/mol. The lower peak potential energy of CO₂ compared with that of CH₄ demonstrated that CO₂ interacted more strongly with coal and was more readily adsorbed at the optimal sites during the CH₄/CO₂ competitive adsorption process. This suggested that CO₂ could quickly occupy a substantial number of adsorption sites, effectively inhibiting CH₄ adsorption. These findings confirmed the efficacy of CO₂ injection for displacing CH₄ in coal seams.

Fig. 11 shows the energy distributions of the CH₄/N₂ mixtures at various ratios. The changes in the potential energy distribution for CH₄/N₂ at different ratios were minimal. The absolute values of the potential energy at the optimal adsorption sites for CH₄ were consistently greater than those for N₂, and the peak value for CH₄ was lower than that for N₂. This indicated that CH₄ occupied the optimal adsorption sites more easily than N₂ across all mixing ratios, reflecting a stronger interaction between coal and CH₄. During competitive adsorption, increasing the proportion of N₂ reduced the CH₄ adsorption and enhanced the N₂ adsorption owing to the quantitative advantage of N₂. However, the gas mixture ratio did not alter the inherent adsorption preference of coal for CH₄ over N₂ because the adsorption sequence CH₄ > N₂ remained unchanged, and the potential energy distribution trend was unaffected. This highlights the importance of the N₂ amount in N₂-ECBM technology for effective CH₄ replacement in coal beds. A well-designed gas injection strategy is crucial for practical applications to achieve efficient CH₄ displacement.

3.3. Interaction energy

The stability of the simulated system is reflected by the interaction energy, which primarily consists of the van der Waals energy, electrostatic energy, and intramolecular energy. Theoretically, an object's internal energy comprises the sum of the kinetic, potential, chemical, ionization, and nuclear energies of its microscopic particles. However, because the molecular, atomic, and nuclear structures of matter remain unchanged during typical thermodynamic state changes, these specific energy changes were not considered in the simulation.

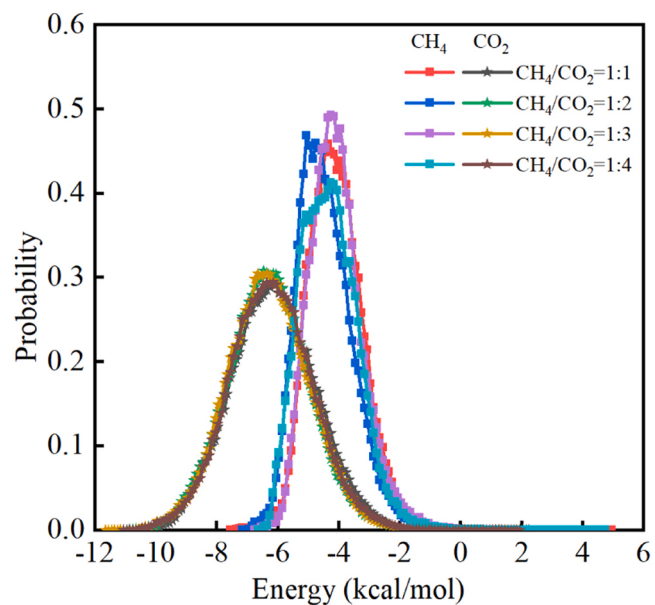


Fig. 10. Potential energy distribution during competitive adsorption of CH₄/CO₂.

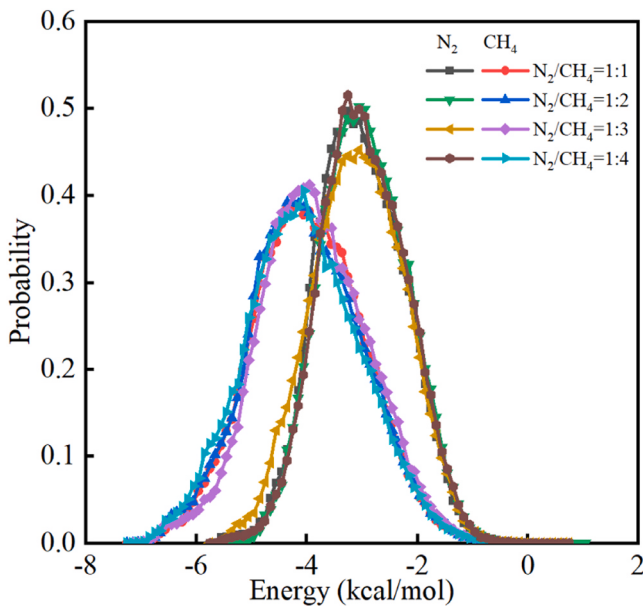


Fig. 11. Potential energy distribution during competitive adsorption of CH_4/N_2 .

Fig. 12 illustrates the variation in interaction energy during CH_4/CO_2 adsorption in coal. The data demonstrated that van der Waals energy dominated the adsorption process, followed by electrostatic energy. As the proportion of CO_2 in the gas mixture increased, both the van der Waals and electrostatic energies initially increased and then decreased, whereas the intramolecular energy continuously decreased. This pattern indicates that during competitive adsorption, many adsorption sites in the coal became occupied, reducing the intermolecular interaction energy and subsequently slowing the adsorption rate.

Fig. 13 illustrates the variation in the interaction energy during the competitive adsorption of the CH_4/N_2 gas mixture in coal. The results revealed that van der Waals energy predominated in the competitive adsorption process, whereas electrostatic energy played a minimal role. A comparison of the energy changes during CH_4/CO_2 and CH_4/N_2 adsorption revealed that the van der Waals and electrostatic energies

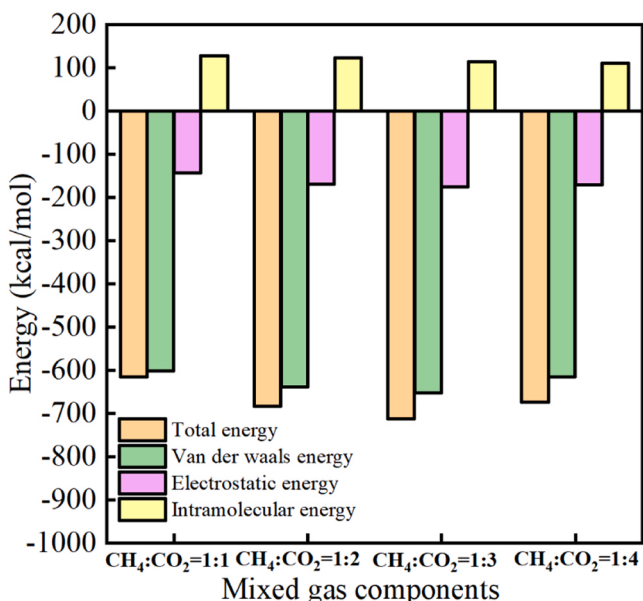


Fig. 12. Distribution of interaction energies during CH_4/CO_2 competitive adsorption.

generated during CH_4/CO_2 adsorption were significantly greater than those during CH_4/N_2 adsorption. The higher adsorption capacity of coal for CH_4/CO_2 is attributed to CO_2 's stronger quadrupole moment and polarization, which enables coal to interact more favorably with CO_2 (Yu et al., 2019).

3.4. Density distribution

Fig. 14 depicts the density distribution of CH_4/CO_2 mixtures at various ratios, providing a visual representation of the gas molecule distribution in coal (Jia et al., 2023a). As the proportion of CO_2 in the mixture increased, the density of CH_4 decreased from 1.861 to 1.153, 0.3819, and 0.2293 g/cm^3 , whereas the density of CO_2 increased from 3.030 to 3.154, 3.168, and 4.289 g/cm^3 , respectively. This indicated that with a higher proportion of CO_2 , the density distribution range of CH_4 in coal diminishes, whereas the range for CO_2 expanded. Across all ratios, the density distribution of CO_2 in coal was consistently larger than that of CH_4 .

Fig. 15 shows the density distribution of the CH_4/N_2 mixtures at various ratios. As the proportion of N_2 in the CH_4/N_2 mixture increased, the density of CH_4 decreased from 1.858 to 1.106 g/cm^3 and then to 0.8107 g/cm^3 , whereas the density of N_2 increased from 0.7066 to 0.7629, 0.7989, and finally to 0.8772 g/cm^3 . This trend indicated that as the N_2 ratio increased, the CH_4 density within the coal cells gradually decreased, and the N_2 density increased. When the CH_4/N_2 ratio was less than 1:4, the CH_4 density was higher than the N_2 density at all ratios. However, at a ratio of 1:4, the N_2 density in the coal cell surpassed that of CH_4 .

In summary, in CH_4/CO_2 and CH_4/N_2 gas mixtures, the density distribution of CH_4 decreased, while that of CO_2 and N_2 increased as their respective proportions increased. The inhibition of CH_4 by CO_2 was more pronounced than that by N_2 owing to differences in the adsorption capacity of coal, which was influenced by the gas properties and structure of the functional groups of coal. The oxygen-containing functional groups in coal favor CO_2 adsorption, whereas the aliphatic functional groups are more conducive to CH_4 and N_2 adsorption (Jia et al., 2023b). Coal contains various functional groups that create distinct adsorption sites for various gases. It is particularly rich in oxygen-containing functional groups such as -OH and R-OH, which facilitate CO_2 adsorption through hydrogen bonding, van der Waals forces, and electrostatic interactions. In contrast, N_2 primarily interacts with the nitrogen-containing functional groups via van der Waals forces. However, the low abundance of nitrogen-containing functional groups in coal and the weak nature of the van der Waals forces render N_2 adsorption less effective. These interactions often require specific conditions such as high temperatures or catalysts to occur efficiently. Consequently, CO_2 injection is more effective than N_2 injection for displacing CH_4 in coal seams during enhanced CBM recovery.

3.5. Adsorption selectivity

Adsorption selectivity is defined as the ratio of the mole fractions of two substances in the adsorbed state to their mole fractions in the free state (Zhang et al., 2015; Zhou et al., 2019; Wu et al., 2017; Jin et al., 2017). This coefficient quantifies the ability of coal to competitively adsorb components of a gas mixture. Calculating the adsorption selectivity provides insights into the competition strength between different gas mixture components and allows the evaluation of the coal's capacity to separate gases. A higher adsorption selectivity indicates greater separation capability. The calculation method is outlined in Eq. (2):

$$S_{ij} = (x_i/x_j)/(y_i/y_j) \quad (2)$$

where x_i denotes the molar proportion of gas i in the adsorbed state; x_j denotes the molar proportion of gas j in the adsorbed state; y_i denotes the molar proportion of gas i in the free state; and y_j denotes the molar

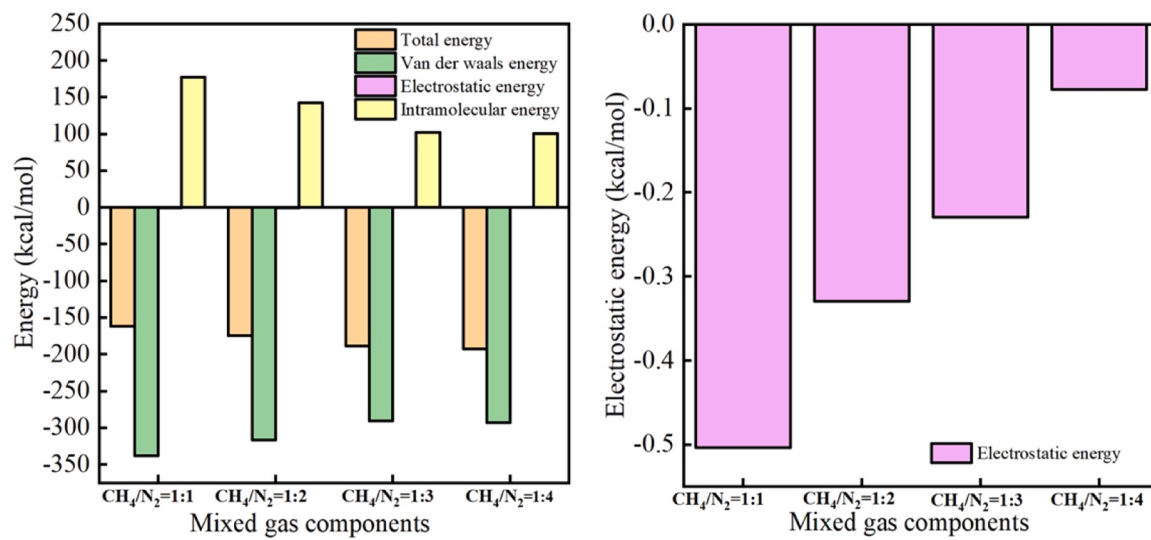


Fig. 13. Distribution of interaction energies during CH₄/N₂ competitive adsorption.

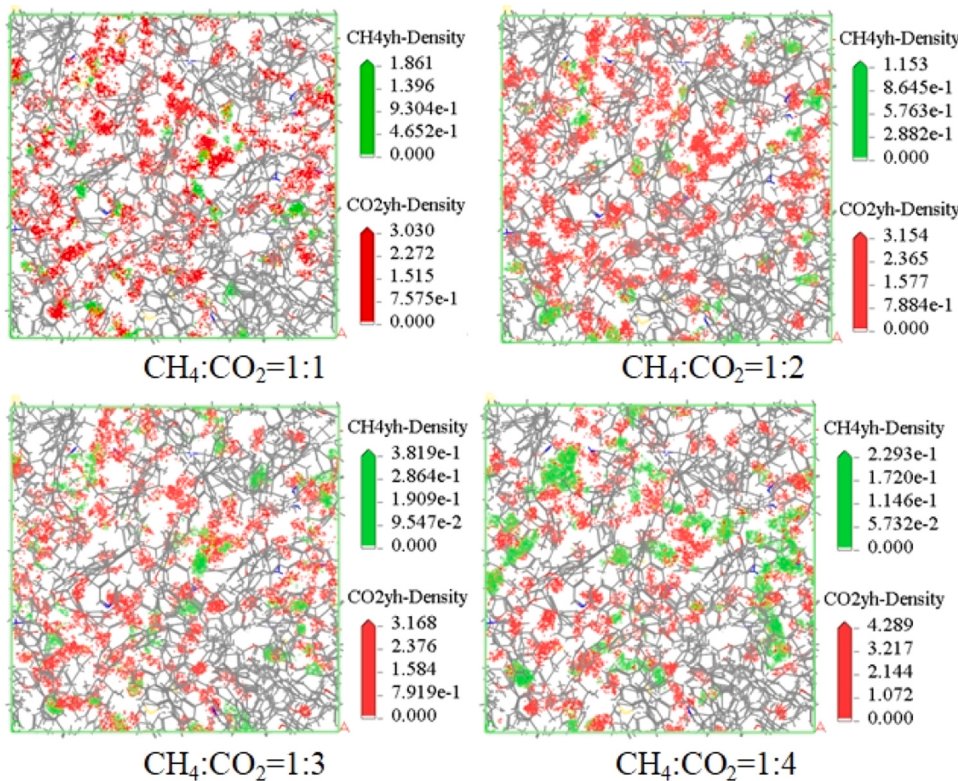


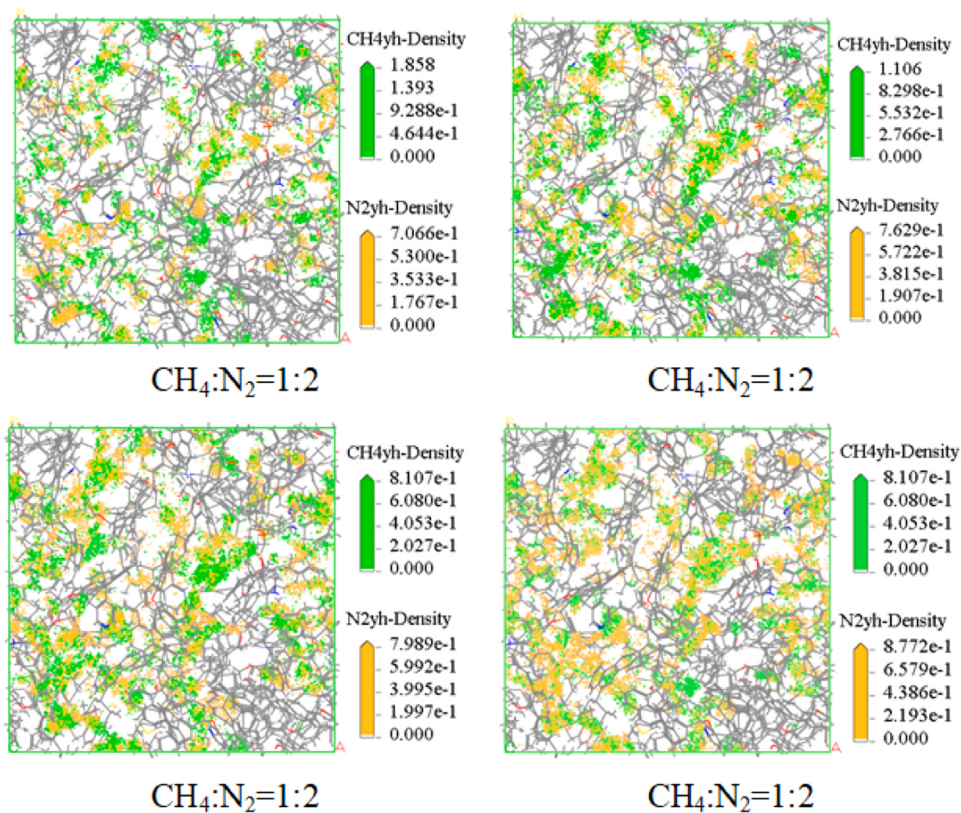
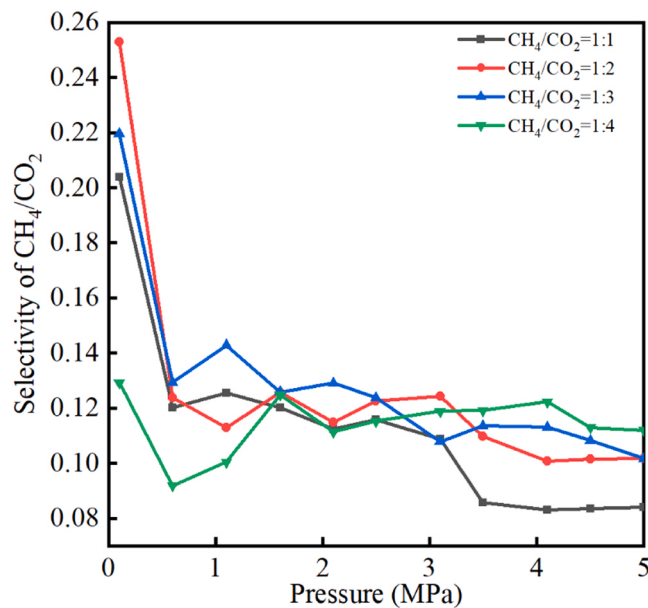
Fig. 14. CH₄/CO₂ density profile.

proportion of gas *j* in the free state. When $S_{ij} > 1$, the adsorption capacity of gas *i* is greater than that of gas *j*. When $S_{ij} = 1$, both gases have equal adsorption capacities. Conversely, when $S_{ij} < 1$, the adsorption capacity of gas *j* is greater than that of gas *i*.

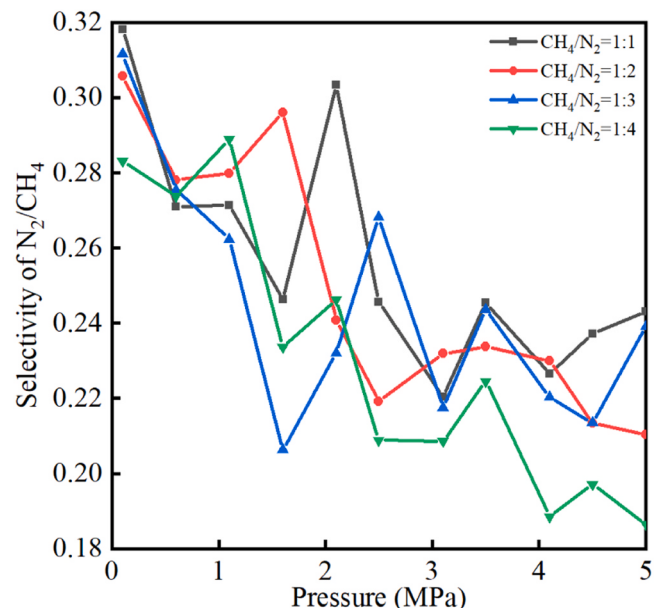
Fig. 16 illustrates the variation in the CH₄/CO₂ adsorption selectivity coefficient with pressure at different mixing ratios. The results demonstrated that the adsorption selectivity of CH₄/CO₂ decreased as the pressure increased, with all selectivity coefficients remaining below 1. This indicates that CO₂ has stronger competitive adsorption ability than CH₄. As the pressure increased, the increased kinetic energy of molecules and the preferential adsorption of CO₂ reduced the number of available adsorption sites, leading to a decline in the adsorption

selectivity of CH₄/CO₂.

Fig. 17 illustrates the variation in the N₂/CH₄ adsorption selectivity coefficient with pressure at different mixing ratios. The results indicated that the selectivity for N₂/CH₄ gradually decreased as the pressure increased, with all selectivity coefficients remaining below 1. This indicated that CH₄ consistently exhibited a stronger competitive adsorption capacity than N₂. However, as the proportion of N₂ increased, it competed with CH₄ for limited adsorption sites owing to its quantitative advantage, leading to a further decline in N₂/CH₄ adsorption selectivity. This highlights the importance of maintaining sufficient N₂ levels during N₂ injection for CH₄ replacement in coal beds to ensure effective displacement.

Fig. 15. CH_4/N_2 density profile.Fig. 16. Adsorption selectivity of CH_4/CO_2 .

In summary, the gas mixture ratio had a minimal effect on the adsorption selectivity coefficient. This was because changes in the mixture ratio did not alter the inherent adsorption strength of coal for individual gases, with the N_2/CH_4 adsorption selectivity coefficient consistently remaining below 1 as the N_2 ratio increased. In gas mixtures, competition between gases may lead to the redistribution of adsorption sites, establishing a new equilibrium without significantly affecting the adsorption selectivity coefficient. Moreover, when

Fig. 17. Adsorption selectivity of N_2/CH_4 .

injecting CO_2 or N_2 to replace CH_4 in coal seams, it is essential to ensure that the concentration of the injected gas is sufficient to facilitate effective gas replacement; otherwise, coalbed methane extraction may be hindered.

3.6. Practical significance

By analyzing the competitive adsorption mechanisms of CH_4/CO_2

and CH_4/N_2 at different mixing ratios, future applications of CO_2 or N_2 injection for CH_4 replacement in coal beds should involve tailoring the gas injection scheme to the specific conditions of coal seams. Selecting the optimal gas concentration is essential to maximize the CH_4 recovery efficiency while simultaneously minimizing the economic costs of coalbed methane extraction.

In CO_2 -ECBM applications, the CO_2 concentration should be maintained at 1–3 times the coal seam gas concentration, as determined by monitoring coal seam gas levels. Within this range, the replacement effect of CO_2 on CH_4 was the most effective. Exceeding this range can lead to CO_2 waste, increased coalbed methane extraction costs, and diminished displacement effects on CH_4 .

In N_2 -ECBM applications, the injected N_2 concentration should be at least three times the coal seam gas concentration, as determined by monitoring coal seam gas levels. Failure to meet this threshold can reduce the effectiveness of CH_4 replacement in coal seams.

4. Conclusion

This study investigated the competitive adsorption characteristics of CH_4/CO_2 and CH_4/N_2 gas mixtures in coal at different ratios, leading to the following conclusions:

- (1) The adsorption sequence of coal for single-component gases was $\text{CO}_2 > \text{CH}_4 > \text{N}_2$. During the competitive adsorption of CH_4/CO_2 and CH_4/N_2 at varying ratios, both CO_2 and N_2 inhibited the CH_4 adsorption, with CO_2 demonstrating a significantly stronger effect. The suppression of CH_4 by N_2 was dependent on its concentration, with a higher N_2 content resulting in greater inhibition. For optimal gas displacement in the CO_2 -ECBM and N_2 -ECBM strategies, the CO_2 concentration should be 1–3 times the methane concentration, whereas the N_2 concentration should be at least three times the methane concentration.
- (2) The proportion of mixed gases had a minimal influence on the potential energy distribution and adsorption selectivity coefficient. Changes in the gas mixture ratio did not affect the coal adsorption sequence of individual gases.
- (3) Van der Waals energy was the primary factor in the competitive adsorption of CH_4/CO_2 and CH_4/N_2 . However, the van der Waals energy of CH_4/CO_2 was approximately twice that of CH_4/N_2 . Additionally, CH_4/CO_2 exhibited significant electrostatic energy, whereas the electrostatic energy of CH_4/N_2 was minimal.
- (4) The density of CH_4 in the CH_4/CO_2 mixture in the same proportion was lower than that in the CH_4/N_2 mixture. This stronger inhibition of CH_4 by CO_2 compared with N_2 was attributed to the stronger interactions between CO_2 and the functional groups in coal, rendering CO_2 more favorable for competitive adsorption.

This study analyzed the competitive adsorption characteristics of CH_4/CO_2 and CH_4/N_2 in anthracite models at different mixing ratios from a molecular perspective. However, the model did not consider the effect of water molecules, despite the significant influence of coal moisture on gas adsorption behavior. Future research should focus on examining how varying the coal moisture content can affect gas adsorption characteristics. Additionally, optimized gas injection strategies for CBM replacement should be developed to accommodate different levels of coal moisture content.

CRediT authorship contribution statement

Jie Wei: Resources. **Haijing Zhang:** Writing – review & editing, Writing – original draft, Investigation. **Xun Zhang:** Resources. **Chaojun Fan:** Methodology, Conceptualization. **Jue Wang:** Resources. **Gang Bai:** Writing – review & editing, Writing – original draft, Methodology, Funding acquisition, Conceptualization. **Yilong Zhang:** Resources.

Declaration of Competing Interest

The authors declare that they have no known competing financial interests or personal relationships that could have appeared to influence the work reported in this paper.

Acknowledgments

This work was financially supported by the Scientific Research Funding project of National Natural Science Foundation of China (52104195, 52274204), Excellent Youth Fund Project of Liaoning Natural Science Foundation (2024JH3/10200042), and China Association for Science and Technology “Young Talent Promotion Project” (2022QNRC001). These supports are gratefully acknowledged. The authors are grateful to the reviewers for discerning comments on this paper.

Notes

The authors declare no competing financial interest.

Appendix A. Supporting information

Supplementary data associated with this article can be found in the online version at [doi:10.1016/j.egyr.2024.12.007](https://doi.org/10.1016/j.egyr.2024.12.007).

Data availability

Data will be made available on request.

References

- Asif, M., Naveen, P., Panigrahi, D.C., Kumar, S., Ojha, k., 2019. Adsorption isotherms of $\text{CO}_2\text{-CH}_4$ binary mixture using IAST for optimized ECBM recovery from sub-bituminous coals of Jharia coalfield: an experimental and modeling approach. *Int. J. Coal Prep. Util.* 39 (8), 403–420. <https://doi.org/10.1080/19392699.2019.1626842>.
- Babatunde, K.A., Negash, B.M., Mojid, M.R., Ahmed, T.Y., Jufar, S.R., 2021. Molecular simulation study of $\text{CO}_2\text{/CH}_4$ adsorption on realistic heterogeneous shale surfaces. *Appl. Surf. Sci.* 543, 148789. <https://doi.org/10.1016/j.apsusc.2020.148789>.
- Bai, G., Su, J., Zhang, Z., Lan, A., Zhou, X., Gao, F., Zhou, J., 2022. Effect of CO_2 injection on CH_4 desorption rate in poor permeability coal seams: an experimental study. *Energy* 238, 121674. <https://doi.org/10.1016/j.energy.2021.121674>.
- Diamond, R., 1957. X-ray diffraction data for large aromatic molecules. *Acta Cryst.* 10 (5), 359–364. <https://doi.org/10.1107/S0365110X5700105X>.
- Dong, K., Zeng, F., Jia, J., Chen, C., Gong, Z., 2019. Molecular simulation of the preferential adsorption of CH_4 and CO_2 in middle-rank coal. *Mol. Simulat.* 45 (1), 15–25. <https://doi.org/10.1080/08927022.2018.1521968>.
- Du, X., Cheng, Y., Liu, Z., Hou, Z., Wu, T., Lei, R., Shu, C., 2020. Study on the adsorption of CH_4 , CO_2 and various CH_4/CO_2 mixture gases on shale. *Alex. Eng. J.* 59 (6), 5165–5178. <https://doi.org/10.1016/j.aej.2020.09.046>.
- Han, J., Bogomolov, A.K., Makarova, E.Y., Yang, Z., Lu, Y., Han, J., Li, X., 2018. Molecular simulation of H_2O , CO_2 , and CH_4 adsorption in coal micropores. *Russ. J. Phys. Chem. B* 12, 714–724. <https://doi.org/10.1134/S199079311804022X>.
- Jia, J., Wang, D., Li, B., Wu, Y., Zhao, D., 2023a. Molecular simulation study on the effect of coal metamorphism on the competitive adsorption of $\text{CO}_2\text{/CH}_4$ in binary system. *Fuel* 335, 127046. <https://doi.org/10.1016/j.fuel.2022.127046>.
- Jia, J., Wu, Y., Zhao, D., Li, B., Wang, D., Wang, F., 2023b. Adsorption of $\text{CH}_4/\text{CO}_2/\text{N}_2$ by different functional groups in coal. *Fuel* 335, 127062. <https://doi.org/10.1016/j.fuel.2022.127062>.
- Jin, Z., Wu, S., Deng, C., Dai, F., 2017. Competitive adsorption behavior and mechanism of different flue gas proportions in coal. *J. China Coal Soc.* 42 (05), 1201–1206. <https://doi.org/10.13225/j.cnki.jccs.2016.0997>.
- Li, Y., Yang, Z., Li, X., 2019. Molecular simulation study on the effect of coal rank and moisture on $\text{CO}_2\text{/CH}_4$ competitive adsorption. *Energy Fuels* 33 (9), 9087–9098. <https://doi.org/10.1021/acs.energyfuels.9b01805>.
- Liu, F., 2023. Impact mechanism of pore topological characteristics to CO_2 -ECBM process in raw coal. *Coal Eng.* 55 (07), 139–144. <https://doi.org/10.11799/ce202307023>.
- Liu, H., Li, Z., Wang, H., Chen, M., Xian, L., 2024. Numerical simulation investigation of N_2 injection for enhanced coalbed methane recovery. *Arab. J. Sci. Eng.* 1–12. <https://doi.org/10.1007/s13369-024-09123-1>.
- Long, H., Lin, H., Yan, M., Bai, Y., Tong, X., Kong, X., Li, S., 2021b. Adsorption and diffusion characteristics of CH_4 , CO_2 , and N_2 in micropores and mesopores of bituminous coal: molecular dynamics. *Fuel* 292, 120268. <https://doi.org/10.1016/j.fuel.2021.120268>.

- Long, H., Lin, H., Yan, M., Chang, P., Li, S., Bai, Y., 2021a. Molecular simulation of the competitive adsorption characteristics of CH₄, CO₂, N₂, and multicomponent gases in coal. *Powder Technol.* 385, 348–356. <https://doi.org/10.1016/j.powtec.2021.03.007>.
- Mcquaid, M.J., Sun, H., Rigby, D., 2004. Development and validation of COMPASS force field parameters for molecules with aliphatic azide chains. *Comput. Chem.* 25 (1), 61–71. <https://doi.org/10.1002/jcc.10316>.
- Meng, J., Zhong, R., Li, S., Yin, F., Nie, B., 2018. Molecular model construction and study of gas adsorption of Zhaozhuang coal. *Energy Fuels* 32 (9), 9727–9737. <https://doi.org/10.1021/acs.energyfuels.8b01940>.
- Ottiger, S., Pini, R., Storti, G., Mazzotti, M., 2008. Measuring and modeling the competitive adsorption of CO₂, CH₄, and N₂ on a dry coal. *Langmuir* 24 (17), 9531–9540. <https://doi.org/10.1021/la801350h>.
- Pini, R., Ottiger, S., Storti, G., Mazzotti, M., 2009. Pure and competitive adsorption of CO₂, CH₄ and N₂ on coal for ECBM. *Energy Procedia* 1 (1), 1705–1710. <https://doi.org/10.1016/j.egypro.2009.01.223>.
- Qu, L., Wang, Z., Liu, L., 2023. Molecular simulation study based on adsorption of gas (CO₂, O₂, CH₄) on Coal. *Fire* 6 (9), 355. <https://doi.org/10.3390/fire6090355>.
- Saghafi, A., Javanmard, H., Pinetown, K., 2014. Study of coal gas wettability for CO₂ storage and CH₄ recovery. *Geofluids* 14 (3), 310–325. <https://doi.org/10.1111/gfl.12078>.
- Shinn, J.H., 1984. From coal to single-stage and two-stage products: a reactive model of coal structure. *Fuel* 63 (9), 1187–1196. [https://doi.org/10.1016/0016-2361\(84\)90422-8](https://doi.org/10.1016/0016-2361(84)90422-8).
- Sun, W., Lin, H., Li, S., Kong, X., Long, H., Yan, M., Bai, Y., Tian, J., 2021. Experimental research on adsorption kinetic characteristics of CH₄, CO₂, and N₂ in coal from Junggar Basin, China, at different temperatures. *Nat. Resour. Res.* 30, 2255–2271. <https://doi.org/10.1007/s11053-021-09812-w>.
- Sun, Y., Zhao, Y., Yuan, L., 2018. CO₂-ECBM in coal nanostructure: modelling and simulation. *Nat. Gas Sci. Eng.* 54, 202–215. <https://doi.org/10.1016/j.jngse.2018.04.007>.
- Sun, Z., Cheng, M., Zhang, W., Jiong, Y., Yu, X., Cui, B., 2022. Molecular simulation of the effect of CO₂/N₂ binary gas on methane adsorption in coal. *Coal Geol. Explor.* 50 (3), 14. (<https://cge.researchcommons.org/journal/vol50/iss3/14>).
- Takanohashi, T., Nakamura, K., Terao, Y., Lino, M., 2000. Computer simulation of solvent swelling of coal molecules: effect of different solvents. *Energy Fuels* 14 (2), 393–399. <https://doi.org/10.1021/ef990147f>.
- Wang, F., Ren, T., Tu, S., Frank, H., Aziz, N., 2012. Implementation of underground longhole directional drilling technology for greenhouse gas mitigation in Chinese coal mines. *Int. J. Greenh. Gas Control* 11, 290–303. <https://doi.org/10.1016/j.ijggc.2012.09.006>.
- Wu, S., Deng, C., Dai, F., 2017. Differences of ability and competitiveness on coal adsorbing CO₂, O₂ and N₂. *J. Environ. Eng.* 11 (7), 4229–4235. <https://doi.org/10.12030/j.cjee.201605044>.
- Wu, S., Jin, Z., Deng, C., 2019b. Molecular simulation of coal-fired plant flue gas competitive adsorption and diffusion on coal. *Fuel* 239, 87–96. <https://doi.org/10.1016/j.fuel.2018.11.011>.
- Wu, S., Deng, C., Wang, X., 2019. Molecular simulation of flue gas and CH₄ competitive adsorption in dry and wet coal. *J. Nat. Gas Sci. Eng.* 71, 102980. <https://doi.org/10.1016/j.jngse.2019.102980>.
- Xiang, J., Zeng, F., Liang, H., Li, B., Song, X., 2014. Molecular simulation of the CH₄/CO₂/H₂O adsorption onto the molecular structure of coal. *Sci. China Earth Sci.* 57 (8), 1749–1759. <https://doi.org/10.1007/s11430-014-4849-9>.
- Xiao, T., Li, S., Long, H., Kong, X., Bai, Y., Qin, A., 2023. Experimental research on adsorption characteristics of N₂, CH₄, and CO₂ in coal under different temperatures and gas pressures. *Energy Sci. Eng.* 11 (2), 637–653. <https://doi.org/10.1002/ese3.1350>.
- Yang, B., Lin, H., Li, S., Yan, M., Long, H., 2021a. Molecular simulation of N₂ and CO₂ injection into a coal model containing adsorbed methane at different temperatures. *Energy* 219, 119686. <https://doi.org/10.1016/j.energy.2020.119686>.
- Yang, R., Liu, S., Wang, H., Lun, Z., Zhou, X., Zhao, C., Min, C., Zhang, H., Xu, Y., Zhang, D., 2021b. Influence of H₂O on adsorbed CH₄ on coal displaced by CO₂ injection: implication for CO₂ sequestration in coal seam with enhanced CH₄ recovery (CO₂-ECBM). *Ind. Eng. Chem. Res.* 60 (43), 15817–15833. <https://doi.org/10.1021/acs.iecr.1c03099>.
- Yang, Z., Yang, S., Han, J., Li, X., Lu, Y., Ji, G., Fu, Q., 2020. Molecular simulation on competitive adsorptions of CO₂, CH₄, and N₂ in deep coal seams. *Chem. Technol. Fuels Oils+* 56, 619–626. <https://doi.org/10.1007/s10553-020-01175-x>.
- You, J., Tian, L., Zhang, C., Yao, H., Dou, W., Fan, B., Hu, S., 2016. Adsorption behavior of carbon dioxide and methane in bituminous coal: a molecular simulation study. *Chin. J. Chem. Eng.* 24 (9), 1275–1282. <https://doi.org/10.1016/j.cjche.2016.05.008>.
- Yu, S., Bo, J., Fengjuan, L., 2019. Competitive adsorption of CO₂/N₂/CH₄ onto coal vitrinite macromolecular: effects of electrostatic interactions and oxygen functionalities. *Fuel* 235, 23–38. <https://doi.org/10.1016/j.fuel.2018.07.087>.
- Zhang, H., Diao, R., Mostofi, M., Evans, B., 2020. Molecular simulation of enhanced CH₄ recovery and CO₂ storage by CO₂-N₂ mixture injection in deformable organic micropores. *J. Nat. Gas Sci. Eng.* 84, 103658. <https://doi.org/10.1016/j.jngse.2020.103658>.
- Zhang, J., Liu, K., Clemnell, M.B., Dewhurst, D.N., Pervukhina, M., 2015. Molecular simulation of CO₂-CH₄ competitive adsorption and induced coal swelling. *Fuel* 160, 309–317. <https://doi.org/10.1016/j.fuel.2015.07.092>.
- Zhao, Y., Feng, Y., Zhang, X., 2016. Selective adsorption and selective transport diffusion of CO₂-CH₄ binary mixture in coal ultramicropores. *Environ. Sci. Technol.* 50 (17), 9380–9389. <https://doi.org/10.1021/acs.est.6b01294>.
- Zheng, S., Yao, Y., Sang, S., Liu, D., Wang, M., Liu, S., 2022. Dynamic characterization of multiphase methane during CO₂-ECBM: an NMR relaxation method. *Fuel* 324, 124526. <https://doi.org/10.1016/j.fuel.2022.124526>.
- Zhou, F., Hussain, F., Cinar, Y., 2013. Injecting pure N₂ and CO₂ to coal for enhanced coalbed methane: experimental observations and numerical simulation. *Int. J. Coal Geol.* 116, 53–62. <https://doi.org/10.1016/j.coal.2013.06.004>.
- Zhou, W., Wang, H., Zhang, Z., Chen, H., Liu, X., 2019. Molecular simulation of CO₂/CH₄/H₂O competitive adsorption and diffusion in brown coal. *RSC Adv.* 9 (6), 3004–3011. <https://doi.org/10.1039/C8RA10243K>.